



Abbas, Y. M., Toyé, A. M., Rubinstein, J. L., & Reithmeier, R. A. F. (2018). Band 3 function and dysfunction in a structural context. *Current Opinion in Hematology*, 25(3), 163-170.
<https://doi.org/10.1097/MOH.0000000000000418>

Peer reviewed version

Link to published version (if available):
[10.1097/MOH.0000000000000418](https://doi.org/10.1097/MOH.0000000000000418)

[Link to publication record in Explore Bristol Research](#)
PDF-document

This is the author accepted manuscript (AAM). The final published version (version of record) is available online via Wolters Kluwer at https://journals.lww.com/co-hematology/Abstract/publishahead/Band_3_function_and_dysfunction_in_a_structural.99339.aspx. Please refer to any applicable terms of use of the publisher.

University of Bristol - Explore Bristol Research

General rights

This document is made available in accordance with publisher policies. Please cite only the published version using the reference above. Full terms of use are available:
<http://www.bristol.ac.uk/pure/about/ebr-terms>

Current Opinion in Hematology

Band 3 Function and Dysfunction in a Structural Context

--Manuscript Draft--

Manuscript Number:	
Full Title:	Band 3 Function and Dysfunction in a Structural Context
Article Type:	Review Article
Corresponding Author:	Reinhart Reithmeier University of Toronto Toronto, Ontario CANADA
Corresponding Author Secondary Information:	
Corresponding Author's Institution:	University of Toronto
Corresponding Author's Secondary Institution:	
First Author:	Reinhart Reithmeier
First Author Secondary Information:	
Order of Authors:	Reinhart Reithmeier
	Yazan Abbas
	John Rubinstein
	Ashley Toye
Order of Authors Secondary Information:	

1 **Band 3 Function and Dysfunction in a Structural Context**

2 Yazan M. Abbas^a, Ashley M. Toye^{b,c}, John L. Rubinstein^{a,d,e} and Reinhart A.F. Reithmeier^{e*}

3

4 ^aHospital for Sick Children Research Institute, Toronto, Ontario, Canada, M5G 0A4

5 ^bSchool of Biochemistry, University of Bristol, Biomedical Sciences Building, Bristol, UK, BS8 1TD

6 ^cBristol Institute of Transfusion Science, NHS Blood and Transplant, Filton, Bristol, UK, BS34 7QH

7 ^dDepartment of Medical Biophysics, University of Toronto, Toronto, Ontario, Canada, M5G 1L7

8 ^eDepartment of Biochemistry, University of Toronto, Toronto, Ontario, Canada, M5S 1A8

9 *To whom to address correspondence: r.reithmeier@utoronto.ca

10

11

12

13

14

15

16 **Purpose of review:** Current research on the human Band 3 glycoprotein, the red cell
17 chloride/bicarbonate anion exchanger (AE1), is highlighted and placed within a structural context.

18 **Recent Findings:** The determination of the crystal structure of the membrane domain of human Band 3,
19 the founding member of the SLC4 family of bicarbonate transporters, is a major breakthrough towards
20 understanding the mechanism of action of this membrane transport protein, its interaction with partner
21 proteins, and how mutations linked to disease affect its ability to fold and function.

22 **Summary:** Band 3 contains 14 transmembrane (TM) segments arranged in a 7+7 TM inverted repeat
23 topology common to all members of the SLC4 family and the unrelated SLC26 anion transporter family.
24 A functional feature of this fold is the presence of a core and a gate domain: the core domain contains
25 two short TM helices (TM3 and 10) that face each other in the middle of the membrane with the positive
26 N-terminal helix dipoles creating the anion binding site, while the gate domain forms the dimer
27 interface. During transport, the movement of these two domains relative to each other provides the
28 intracellular and extracellular compartments with alternating access to the central anion binding site.

29 **Keywords:** anion transport, Band 3, membrane proteins, SLC4, trafficking

30

31

32 **Introduction**

33 Band 3, also known as Anion Exchanger 1 (AE1) or Solute Carrier 4A1 (SLC4A1), is responsible for
34 the electroneutral exchange of chloride and bicarbonate across the red cell membrane, a process
35 necessary for efficient transport of CO₂ during respiration. Band 3 is also important for maintaining red
36 cell shape, anchoring the actin-spectrin cytoskeleton at the membrane. A truncated kidney anion
37 exchanger 1 (kAE1), lacking the first 65 residues, is expressed in the basolateral membrane of α -
38 intercalated cells, where it plays a role in bicarbonate reabsorption into the blood to facilitate acid
39 secretion into the urine. Genetic defects in the *SLC4A1* gene lead to red blood cell diseases, which
40 include hereditary spherocytosis (HS), hereditary stomatocytosis (HSt), and Southeast Asian
41 ovalocytosis (SAO), as well as the kidney disease distal renal tubular acidosis (dRTA).

42 Human Band 3 is an abundant 911-residue glycoprotein comprised of two domains: an N-terminal
43 cytosolic domain (cdAE1) that anchors the cytoskeleton at the membrane and interacts with numerous
44 erythrocyte proteins including deoxyhemoglobin [1] and a C-terminal membrane domain (mdAE1) that
45 performs anion exchange [2]. Through a cytosolic C-terminal tail, the membrane domain interacts with
46 carbonic anhydrase II (CAII), which interconverts carbon dioxide and bicarbonate, to form a bicarbonate
47 transport metabolon [3,4]. Band 3 exists as a mixture of dimers and tetramers in membranes and
48 detergent solutions [5]. These oligomers form interaction hubs around which integral and peripheral
49 membrane proteins of the red blood cell are organized [6].

50 A variety of methods have been used to elucidate the transmembrane topology of Band 3, including
51 proteolysis, chemical labeling, epitope mapping, scanning N-glycosylation and cysteine mutagenesis,
52 and fragment-complementation assays [7**]. While these experiments indicated that mdAE1 crosses the
53 membrane up to 14 times, the topology around putative spans 9 to 12 remained unclear. The crystal

54 structure of cdAE1 was determined in 2000 [1], but mdAE1 resisted high-resolution structural analysis
55 for a further 15 years [8**]. Crystallization of dimeric human mdAE1 (Fig. 1) was enabled by trypsin
56 cleavage and deglycosylation, use of a monoclonal Fab that bound a conformational epitope, and
57 locking of the structure in an outward-facing open conformation with H₂DIDS, a competitive inhibitor
58 of anion transport.

59 **The membrane domain of Band 3 has a 7+7 TM inverted repeat structure**

60 The crystal structure of mdAE1 confirmed that Band 3 contains 14 α -helical transmembrane (TM)
61 segments that consist of two inverted seven TM-repeats (TM1 to 7 and TM8 to 14) (Fig. 2a). The TM
62 segments have a complex topology and are intertwined to form two sub-domains: the core and gate
63 domains (Fig. 2b). TM1 to 4 and 8 to 11 make up the core domain, and TM5 to 7 and 12 to 14 the gate
64 domain (Fig. 2c). This folding pattern, known as the 7+7 TM inverted repeat fold [9*], differs from the
65 major facilitator superfamily (MFS) of transporters that have a much simpler 12 TM topology arranged
66 in two linear domains (TM1-6 and TM7-12) connected by a cytosolic linker [10,11*]. The 7+7 TM
67 inverted repeat topology appears to be common to the SLC4 family proteins, as suggested by recent
68 structures of proteins related to human SLC4A11 [12*,13*]. This fold was first observed in the bacterial
69 proton-uracil symporter UraA, a member of the SLC23 nucleobase transport family [14*], and
70 subsequently in the fungal proton-purine symporter UapA [15*] and a bacterial SLC26 anion transporter
71 [16*].

72 **Helix dipoles comprise the anion binding site**

73 A unique feature of 7+7 TM inverted repeat proteins is the presence of two pseudo-symmetry related
74 half-helices, TM3 and TM10, that face each other in the middle of the lipid bilayer [9*]. In UraA and
75 UapA, substrates are bound between the N termini of these two half-helices [14*,15*]. In mdAE1, the

76 anion-binding site is also found between the N-terminal ends of TM3 and 10 located in the core domain
77 (Fig. 3a). The anion is held in place by the positive helical dipoles [17]. Transport also involves Arg730
78 from TM10 and Glu681 from TM8 (Fig. 3a). Arg730 forms part of the anion-binding site and interacts
79 with one of the sulfates of H₂DIDS, while Glu681 points towards the anion-binding site and may act as
80 an anionic gate. Consistent with this mode of substrate binding, mutation of Arg748 in mouse Band 3
81 (equivalent to Arg730) impairs anion transport [18]. Of note, Glu681 has been identified as the proton-
82 binding site for proton-sulfate/chloride exchange by Band 3 [19]. In the sodium-bicarbonate co-
83 transporting members of the SLC4 family, Glu681 is replaced by Asp, suggesting that this Asp likely
84 provides the sodium-binding site in these proteins [20].

85 **Disease-causing Band 3 mutations**

86 The crystal structure of mdAE1 revealed the location of a variety of mutations that cause the diseases
87 HS, HSt, and dRTA [7**]. Many of these mutations cause misfolding and/or aberrant trafficking of the
88 protein, affecting Band 3 localisation during red cell development or targeting to the basolateral surface
89 of kidney epithelial cells. While most mutations cause standalone trafficking defects that impact only
90 one allele and lead to recessive disease, some mutations can lead to mis-trafficking of the wild type
91 protein by hetero-dimerization causing a dominant disease phenotype [7**]. Band 3 trafficking is also
92 influenced by additional factors, including Glycophorin A (GPA) and ER chaperones. GPA facilitates
93 trafficking of Band 3 to the cell surface and can rescue certain Band 3 mutants, including Band 3 SAO
94 [21]. ER chaperones involved in the folding of glycoproteins, like calnexin, are selectively removed
95 during terminal erythropoiesis while inhibition of these chaperones in kidney cells can rescue trafficking
96 of certain kAE1 mutants [22,23]. Specific mutations in Band 3 can cause HSt by inducing cation
97 passage in the protein; many of these mutations are clustered at the interface between the core and gate
98 domains near the anion binding site (Fig. 3b) [7**].

99 **Ion transport mechanism of mdAE1**

100 The core and gate domains are separated by a V-shaped cleft that opens to the extracellular side of the
101 membrane (Fig. 4a). The substrate-binding site lies at the vertex of the cleft (Fig. 4a), and substrate
102 passage to this region is blocked when the inhibitor H₂DIDS is bound (Fig. 2c). Substrate binding
103 residues are exclusively in the core domain (Fig. 3a), while the DIDS-reactive Lys539 and Lys851 are in
104 the gate domain on TM5 and 13, respectively (Fig. 2c).

105 Anion exchange is achieved through a relative movement of the core and gate domains, providing the
106 substrates with alternating access to either side of the membrane [24]. While the precise mechanism of
107 anion transport remains unclear, there are three prevailing models for alternating access (Fig. 4b) [25].
108 In the “rocking switch model” both core and gate domains move relative to the lipid bilayer to provide
109 the alternating access. In the “rocking bundle model” alternating access is accomplished through the
110 movement of one of the domains against the other, which remains immobile. Finally, in the “elevator
111 transport model” one domain moves against the other to change the depth of the substrate-binding site in
112 the membrane. Structures of other 7+7 TM inverted repeat transporters showed that they adopt inward-
113 facing or intermediate occluded conformations, in contrast to the outward-facing mdAE1
114 [12*,13*,14*,15*,16*,26**]. Thus far, the structure of only one member of the 7+7 TM inverted repeat
115 family, UraA, has been reported in two states: inward-facing and occluded [26**]. Comparison of these
116 two conformations suggests a hybrid rocking-bundle elevator mode of transport, in which alternating
117 access is achieved through a combination of a relative movement of the core against the gate, local
118 rearrangement within the gate, and concomitant translocation of the substrate. However, a model of
119 inward-facing mdAE1 built using a technique known as repeat-swap homology modelling, in which the
120 conformation of the two pseudo-symmetry related repeats are exchanged [27*,28], suggests that mdAE1

121 uses only an elevator-like mechanism for anion transport. Further experiments are needed to discern
122 between the possible modes of transport by mdAE1 and related family members.

123 **The crystal structure provides context for other functional elements of Band 3**

124 The N- and C-terminal regions of mdAE1 are in the cytoplasm and contain two amphipathic α -helices,
125 H1 and H6, that lie along the inner membrane surface (Fig. 4c). H1 (residues 383-401) precedes TM1,
126 connecting the transmembrane region to the cytosolic domain of Band 3. A nine-amino acid deletion
127 (Ala401-Ala409) in this region causes SAO [29], potentially altering the relative orientation of the
128 cytoplasmic and membrane domains. H6 follows TM14 and links it to the C-terminal CAII-interacting
129 region of Band 3.

130 The membrane domain of AE1 contains four additional amphipathic α -helices (H2-H5) that connect TM
131 segments (Fig. 4c). H2 lies on the cytoplasmic face of mdAE1 between TM4 and 5 and H3 lies on the
132 extracellular side between TM11 and 12. Both H2 and H3 connect the core to the gate domain, and the
133 repeat-swap homology model of inward-facing mdAE1 suggests that H2 and H3 undergo a
134 rearrangement to facilitate mdAE1 conformational changes during anion transport [27*].

135 The mdAE1 and cdAE1 can be separated by mild protease treatment of red cell ghosts and are thought
136 to function independently [2], unlike other SLC4 proteins in which the cytoplasmic domain is required
137 for activity [30,31]. Analysis of purified bovine Band 3 by negative-stain electron microscopy suggested
138 that the membrane domain and cytosolic domain are connect by a 3 nm flexible linker [32*]. In contrast,
139 a model of full-length human Band 3 based on the crystal structures of mdAE1, cdAE1, and zero-length
140 cross-linking analysis of red blood cell membranes suggested a more compact arrangement within the
141 intact protein, as well as an interaction between cytoplasmic loops of the membrane domain and the
142 cytosolic domain [33*]. This interaction is proposed to hold the cytosolic domain in place and out of the

143 way of the substrate exit pore on the cytoplasmic side of mdAE1 [33*], supporting the notion that Band
144 3 does not contain a substrate access tunnel in its cytosolic domain [34].

145 Interestingly, the presence of a discontinuous SH2 domain in Band 3 that regulates anion transport by a
146 phosphorylation-dependent mechanism was reported recently [35**]. A conserved phospho-tyrosine
147 binding motif was detected within H2 that interacts with phosphorylated cdAE1, disrupting Band 3-
148 cytoskeletal interactions and destabilizing the red blood cell membrane. This intramolecular
149 rearrangement would require that H2 partially unfolds to interact with phosphorylated cdAE1, and is
150 consistent with the notion that H2, which links the core and gate domains, is involved in conformational
151 changes associated with anion transport [27*]. Using Syk kinase inhibitors to prevent tyrosine
152 phosphorylation of Band 3 and increase erythrocyte membrane strength reduced *Plasmodium falciparum*
153 egress in parasitized red blood cells, thus providing a potential therapeutic avenue to inhibit malaria
154 progression [36].

155 **Band 3 dimer and tetramer structures**

156 The structure of mdAE1 showed that dimerization is mediated exclusively by the gate domain, through
157 interactions between TM5 and 6 from each subunit, and some residues from TM7, H4, and the loop
158 connecting H4 to H5 (Fig. 1). Interfacial lipids have been shown to be important for oligomerization of
159 many membrane proteins [37*] but their role in stabilization of the Band 3 dimer is unclear. While both
160 UraA and UapA require dimerization for transport activity [15*,26**], studies with inhibitors have
161 shown that each subunit of Band 3 can operate independently [38]. Indeed, co-expression of wild-type
162 Band 3 and a non-functional SAO Band 3 mutant results in the surface expression of a heterodimer that
163 retains almost 50% of wildtype activity [29]. Furthermore, it has been shown that the region around
164 TM6-7, which is involved in dimerization, was dispensable for Band 3 function [39,40].

165 Band 3 tetramers are dimers of dimers stabilized by binding of ankyrin to each tetramer [5,41]. Cross-
166 linking analysis provides a model for Band 3 tetramer formation involving Glu272 and Lys353 from the
167 cytosolic domains, and revealed a large interaction interface between Band 3 and ankyrin [33*].
168 Additionally, this analysis showed that GPA interacts with cdAE1 [33*], which also interacts with
169 Glu658 in TM8/9 of mdAE1 to create the Wright blood group antigen [42]. Additional interactions were
170 proposed for cytosolic loops of mdAE1 with protein 4.1 and protein 4.2, two adaptor proteins involved
171 in maintaining cytoskeletal interactions. However, the significance of protein 4.2-mdAE1 associations
172 are unclear as an enhancement effect on Band 3 anion exchange by protein 4.2 was only observed in the
173 presence of the Band 3 N terminus that contains the main protein 4.2 binding site [43].

174 **Band 3 is a protein interaction hub**

175 The human Band 3 tetrameric macro/multiprotein complex, known as the Band 3 complex in early
176 literature, consists of a tetramer of Band 3 bound to ankyrin, protein 4.2, and GPA. Ankyrin and protein
177 4.2 binding to Band 3 facilitates its association to the erythrocyte spectrin cytoskeleton. The Rhesus
178 protein sub-complex comprising Rh, RhAG, LW, CD47, and Glycophorin B has also been shown to
179 associate with the tetrameric complex [44]. In contrast, dimeric Band 3 is thought to be either freely
180 mobile in the membrane or associated within an actin-junctional complex, the composition of which
181 varies between species [44]. In humans, this junctional complex consists of Band 3 dimers, protein 4.1,
182 adducin, dematin, GPC, p55, Rh, and also GLUT1 [44,45].

183 Several of the integral and peripheral membrane proteins that associate with Band 3 also influence its
184 function and/or trafficking, such as GPA, which affects both [21]; carbonic anhydrase II, which forms a
185 metabolon with Band 3 [3]; stomatin, which increased Band 3 transport activity [46]; and protein 4.2,
186 which increased Band 3-specific chloride influx in *Xenopus* oocytes [43] but decreased activity in

187 reconstituted liposomes [47]. Of note, Aquaporin-1 was recently reported to interact with Band 3 [48],
188 suggesting the existence of a super-complex involving Band 3, deoxyhemoglobin, CAII, and aquaporin-
189 1 to channel substrates to and from the transporters and their cognate enzyme. How Band 3 associates
190 with so many proteins, and which regions of Band 3 are involved, still needs to be fully delineated.
191 However, with many copies of Band 3 (1.2×10^6) available in each cell it is likely that there are many
192 flavours of Band 3 complexes.

193 **Future prospects**

194 The crystal structures of cdAE1 and mdAE1 have provided valuable molecular insights into Band 3
195 function and dysfunction, yet the molecular mechanism of substrate transport and Band 3's interaction
196 with other proteins remains elusive. Structures of the inward-facing state of mdAE1 would reveal the
197 extent of the conformational changes associated with transport. A high-resolution structure of intact
198 Band 3 is needed to show the relative orientation of cytosolic and membrane domains and studies of the
199 dynamics of this interaction are needed. Single-particle electron cryo-microscopy (cryo-EM), in
200 particular, holds considerable promise as recent improvements in microscopes and image processing
201 have led to high-resolution structures of complex membrane transport systems [49,50]. Molecular
202 dynamics (MD) simulations of Band 3 in complex lipid bilayers will allow the conformational changes
203 associated with transport to be modelled in a membrane environment [7**]. MD simulations have
204 recently been used to determine the dynamics the Band 3 TM1 signal-anchor that is responsible for
205 integrating the protein into the ER membrane [51]. Finally, the Band 3 structure has been used to build
206 models of other members of the human SLC4 and SLC26 transporter families and to understand the
207 effect of disease-causing mutations on protein folding and function [7**,52*,53, 54]. We can now look
208 forward to the challenge of determining how this transporter works at the molecular level and how it

209 interacts with the cytoskeleton, GPA, and a multitude of other membrane proteins to build a dynamic
210 cellular model of Band 3 in action.

211 **Key Points**

- 212 • The structure of the membrane domain of human Band 3 has revealed the molecular details of the
213 substrate-binding site and possible mechanisms of anion transport.
- 214 • The structure of human Band 3 has allowed localization of disease-causing mutations and
215 determination of their effect on protein folding and function.
- 216 • Models of related SLC4 and 26 transport proteins can be built using the structure of human Band 3
217 as a template.
- 218 • The structure of intact Band 3 still needs to be determined in order to establish the relationship
219 between the cytoplasmic and membrane domains.
- 220 • Band 3 does not operate in isolation but as part of a multi-protein complex integral to the integrity
221 and function of the red blood cell.

222

223 **Figure Legends**

224 **Figure 1. Structure of dimeric of mdAE1.** (a-b) Cartoon representation of mdAE1 (PDB ID: 4YZF)
225 viewed along the plane of the membrane, with H₂DIDS removed from the model. The 14 TM helices are
226 coloured from N-terminus (blue) to C-terminus (red). The dimerization interface is indicated by
227 asterisks, the anionic substrate by a purple sphere, and substrate passage within subunit B with a grey
228 arrow.

229 **Figure 2. Structure and topology of monomeric mdAE1** (a) The core domain comprises TM1 to 4
230 from repeat 1 and TM8 to 11 from repeat 2, which can be superposed on top of each other, while the
231 gate domain is made up of TM5 to 7 from repeat 1 and TM12 to 14 from repeat 2, which also superpose
232 well. The TMs and repeats are normally intertwined, but in this figure they are separated for clarity and
233 the pseudo-symmetry rotation axis is shown (gray circle and arrow). (b) Topology diagram of mdAE1
234 coloured as in (a). mdAE1 contains a single N-linked glycosylation site at Asn642. (c) Close-up view of
235 mdAE1 viewed from the extracellular space showing the core and gate domains, with K539 and K851,
236 from TM5 and 13 respectively, and the crosslinking H₂DIDS represented as sticks.

237 **Figure 3. Key residues in the substrate binding site and localization of some disease-causing**
238 **mutations.** (a) Close-up view of the mdAE1 substrate binding site formed at the N-termini of TM3 and
239 TM10, which meet in the center of the protein near the middle of the membrane. R730 interacts with one
240 of the sulfates (*) from H₂DIDS. (b) Cartoon loop representation of mdAE1 in the same orientation as
241 Fig. 2c. Residues mutated in Hereditary Stomatocytosis that induce a cation leak in mdAE1 are
242 represented by pink spheres. Most of the mutations cluster around the interface of the core and gate
243 domains of the protein, including within TM10 close to the substrate-binding site.

244 **Figure 4. The mdAE1 structure provides additional context for Band 3 function.** (a) Cross-section
245 of mdAE1 subunit A (wheat surface colour with grey interior). R730 lies at the vertex of the V-shaped
246 substrate-binding cleft that is open to the extracellular environment. (b) Schematic of possible
247 membrane transport mechanisms that allow the molecule to alternate between outward-open and inward-
248 open conformations to provide the substrate (purple sphere) with access to different sides of the
249 membrane. Yellow arrows indicate domain movements. (c) Cartoon representation of mdAE1 subunit A
250 with amphipathic α -helices that lie parallel to the membrane (H1-H6) colored as in Fig. 1a.

251

252 **References**

- 253 1. Zhang D, Kiyatkin A, Bolin JT, Low PS: **Crystallographic structure and functional**
254 **interpretation of the cytoplasmic domain of erythrocyte membrane band 3.** *Blood* 2000,
255 **96:2925–2933.**
- 256 2. Grinstein S, Ship S, Rothstein A: **Anion transport in relation to proteolytic dissection of band**
257 **3 protein.** *Biochim. Biophys. Acta* 1978, **507:294–304.**
- 258 3. Sterling D, Reithmeier RA, Casey JR: **A transport metabolon. Functional interaction of**
259 **carbonic anhydrase II and chloride/bicarbonate exchangers.** *Journal of Biological Chemistry*
260 2001, **276:47886–47894.**
- 261 4. Moraes TF, Reithmeier RAF: **Membrane transport metabolons.** *Biochim. Biophys. Acta* 2012,
262 **1818:2687–2706.**
- 263 5. Van Dort HM, Moriyama R, Low PS: **Effect of Band 3 Subunit Equilibrium on the Kinetics**
264 **and Affinity of Ankyrin Binding to Erythrocyte Membrane Vesicles.** *Journal of Biological*
265 *Chemistry* 1998, **273:14819–14826.**
- 266 6. Lux SE: **Anatomy of the red cell membrane skeleton: unanswered questions.** *Blood* 2016,
267 **127:187–199.**
- 268 7. Reithmeier RAF, Casey JR, Kalli AC, Sansom MSP, Alguel Y, Iwata S: **Band 3, the human red**
269 **cell chloride/bicarbonate anion exchanger (AE1, SLC4A1), in a structural context.** *Biochim.*
270 *Biophys. Acta* 2016, **1858:1507–1532.**
- 271 ** A review summarizing 50 years of research on human Band 3 in the light of the crystal structure
272 of the membrane domain and localization of disease-causing mutations in the protein structure.
- 273 8. Arakawa T, Kobayashi-Yurugi T, Alguel Y, Iwanari H, Hatae H, Iwata M, Abe Y, Hino T, Ikeda-
274 Suno C, Kuma H, et al.: **Crystal structure of the anion exchanger domain of human**
275 **erythrocyte band 3.** *Science* 2015, **350:680–684.**
- 276 ** Crystal structure of human Band 3 membrane domain reveals 7+7 TM inverted repeat topology,
277 key features of the anion binding site, and how the membrane domain dimerizes.
- 278 9. Chang Y-N, Geertsma ER: **The novel class of seven transmembrane segment inverted repeat**
279 **carriers.** *Biological Chemistry* 2017, **398:165–174.**
- 280 * Review highlights common 7+7 inverted repeat topology of the SLC4, SLC23 and SLC26
281 families of membrane transport proteins and transport mechanism involving rigid domain
282 movements and a vertical translocation and rotation of the core domain relative to a gate domain
283 at the dimer interface in agreement with an elevator mechanism.
- 284 10. Abramson J, Kaback HR, Iwata S: **Structural comparison of lactose permease and the**
285 **glycerol-3-phosphate antiporter: members of the major facilitator superfamily.** *Curr Opin*
286 *Struct Biol* 2004, **14:413–419.**

- 287 11. Quistgaard EM, Löw C, Guettou F, Nordlund P: **Understanding transport by the major**
288 **facilitator superfamily (MFS): structures pave the way.** *Nat Rev Mol Cell Biol* 2016,
289 **17:nrm.2015.25–132.**
- 290 * The increased availability of crystal structures of MFS transporters has provided insight into the
291 conformational changes associated with transport.
- 292 12. Thurtle-Schmidt BH, Stroud RM: **Structure of Bor1 supports an elevator transport**
293 **mechanism for SLC4 anion exchangers.** *Proceedings of the National Academy of Sciences*
294 2016, **113**:10542–10546.
- 295 * Crystal structure of plant Bor1p in the inward-facing state and modeling suggests a rotation and
296 translation of the core domain relative to the gate domain at the dimer interface, supporting and
297 elevator-like mechanism for SLC4 proteins.
- 298 13. Coudray N, L Seyler S, Lasala R, Zhang Z, Clark KM, Dumont ME, Rohou A, Beckstein O,
299 Stokes DL: **Structure of the SLC4 transporter Bor1p in an inward-facing conformation.**
300 *Protein Science* 2016, **26**:130–145.
- 301 * The determination of the structure of Bor1p, a yeast borate transporter, in the inward-facing
302 conformation combined with molecular dynamics simulations in comparison to the Band 3
303 structure suggest rigid body movement of the core domain relative to the gate domain in a
304 rocking-bundle type mechanism.
- 305 14. Lu F, Li S, Jiang Y, Jiang J, Fan H, Lu G, Deng D, Dang S, Zhang X, Wang J, et al.: **Structure**
306 **and mechanism of the uracil transporter UraA.** *Nature* 2011, **472**:243–246.
- 307 * First crystal structure of a 7+7 TM inverted repeat membrane transport protein, bound to substrate
308 and in an inward-facing conformation.
- 309 15. Alguel Y, Amillis S, Leung J, Lambrinidis G, Capaldi S, Scull NJ, Craven G, Iwata S, Armstrong
310 A, Mikros E, et al.: **Structure of eukaryotic purine/H⁺ symporter UapA suggests a role for**
311 **homodimerization in transport activity.** *Nat Commun* 2016, **7**:ncomms11336.
- 312 * First structure of a dimeric SLC23 protein revealing a role for dimerization in transport activity.
- 313 16. Geertsma ER, Chang Y-N, Shaik FR, Neldner Y, Pardon E, Steyaert J, Dutzler R: **Structure of a**
314 **prokaryotic fumarate transporter reveals the architecture of the SLC26 family.** *Nat Struct*
315 *Mol Biol* 2015, **22**:803–808.
- 316 * First crystal structure of a member of the SLC26 family of anion transport membrane protein
317 reveals a 7+7 inverted repeat topology.
- 318 17. He JJ, Quijcho FA: **Dominant role of local dipoles in stabilizing uncompensated charges on a**
319 **sulfate sequestered in a periplasmic active transport protein.** *Protein Science* 1993, **2**:1643–
320 1647.
- 321 18. Karbach D, Staub M, Wood PG, Passow H: **Effect of site-directed mutagenesis of the arginine**

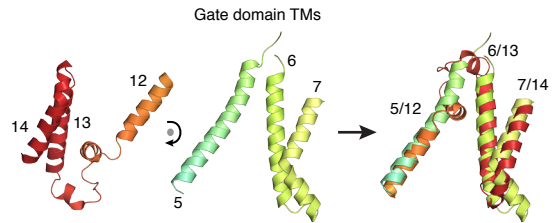
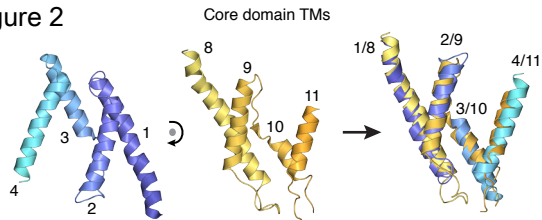
- 322 **residues 509 and 748 on mouse band 3 protein-mediated anion transport.** *BBA -*
323 *Biomembranes* 1998, **1371**:114–122.
- 324 19. Jennings ML, Smith JS: **Anion-proton cotransport through the human red blood cell band 3**
325 **protein. Role of glutamate 681.** *Journal of Biological Chemistry* 1992, **267**:13964–13971.
- 326 20. Kurtz I, Zhu Q: **Structure, function, and regulation of the Slc4 Nbce1 transporter and its role**
327 **in causing proximal renal tubular acidosis.** *Current Opinion in Nephrology and Hypertension*
328 2013, **22**:572–583.
- 329 21. Williamson RC, Toyé AM: **Glycophorin A: Band 3 aid.** *Blood Cells, Molecules, and Diseases*
330 2008, **41**:35–43.
- 331 22. Patterson ST, Reithmeier RAF: **Cell surface rescue of kidney anion exchanger 1 mutants by**
332 **disruption of chaperone interactions.** *J. Biol. Chem.* 2010, **285**:33423–33434.
- 333 23. Patterson ST, Li J, Kang J-A, Wickrema A, Williams DB, Reithmeier RAF: **Loss of specific**
334 **chaperones involved in membrane glycoprotein biosynthesis during the maturation of**
335 **human erythroid progenitor cells.** *Journal of Biological Chemistry* 2009, **284**:14547–14557.
- 336 24. Jardetzky O: **Simple Allosteric Model for Membrane Pumps.** *Nature* 1966, **211**:969–970.
- 337 25. Drew D, Boudker O: **Shared Molecular Mechanisms of Membrane Transporters.** *Annu Rev*
338 *Biochem* 2016, **85**:543–572.
- 339 26. Yu X, Yang G, Yan C, Baylon JL, Jiang J, Fan H, Lu G, Hasegawa K, Okumura H, Wang T, et
340 al.: **Dimeric structure of the uracil:proton symporter UraA provides mechanistic insights**
341 **into the SLC4/23/26 transporters.** *Cell Res* 2017, **27**:1020–1033.
- 342 ** An update to the crystal structure of UraA supports a functional dimeric structure formed by
343 interaction of the gate domain. Furthermore, comparison of the occluded conformation of UraA
344 determined in this study to the previously determined inward-open conformation reveals that
345 UraA, and possibly other SLC4/23/26 transporters, utilize a transport mechanism with rocking-
346 bundle and elevator-like motions accompanied by local rearrangement within the gate domain.
- 347 27. Ficici E, Faraldo-Gómez JD, Jennings ML, Forrest LR: **Asymmetry of inverted-topology**
348 **repeats in the AE1 anion exchanger suggests an elevator-like mechanism.** *The Journal of*
349 *General Physiology* 2017, **264**:jgp.201711836.
- 350 * Homology modelling of the inward-facing state mdAE1 using the outward-facing state of the
351 mdAE1 crystal structure suggests an elevator-type movement of the core domain relative to the
352 stationary gate domain at the dimer interface.
- 353 28. Vergara-Jaque A, Fenollar-Ferrer C, Kaufmann D, Forrest LR: **Repeat-swap homology**
354 **modeling of secondary active transporters: updated protocol and prediction of elevator-type**
355 **mechanisms.** *Front. Pharmacol.* 2015, **6**:610.
- 356 29. Jennings ML, Gosselink PG: **Anion Exchange Protein in Southeast Asian Ovalocytes:**

- 357 **Heterodimer Formation between Normal and Variant Subunits.** *Biochemistry* 1995,
358 **34:3588–3595.**
- 359 30. Stewart AK, Chernova MN, Shmukler BE, Wilhelm S, Alper SL: **Regulation of AE2-mediated**
360 **Cl⁻ transport by intracellular or by extracellular pH requires highly conserved amino acid**
361 **residues of the AE2 NH2-terminal cytoplasmic domain.** *The Journal of General Physiology*
362 2002, **120:707–722.**
- 363 31. Loganathan SK, Lukowski CM, Casey JR: **The cytoplasmic domain is essential for transport**
364 **function of the integral membrane transport protein SLC4A11.** *Am. J. Physiol., Cell Physiol.*
365 2016, **310:C161–74.**
- 366 32. Jiang J, Magilnick N, Tsirulnikov K, Abuladze N, Atanasov I, Ge P, Narla M, Pushkin A, Zhou
367 ZH, Kurtz I: **Single Particle Electron Microscopy Analysis of the Bovine Anion Exchanger 1**
368 **Reveals a Flexible Linker Connecting the Cytoplasmic and Membrane Domains.** *PLoS ONE*
369 2013, **8:e55408.**
- 370 * First structure of an intact Band 3 protein showing the relative orientations of the cytoplasmic and
371 membrane domains.
- 372 33. Rivera-Santiago R, Harper SL, Sriswasdi S, Hembach P, Speicher DW: **Full-Length Anion**
373 **Exchanger 1 Structure and Interactions with Ankyrin-1 Determined by Zero Length**
374 **Crosslinking of Erythrocyte Membranes.** *Structure* 2017, **25:132–145.**
- 375 * Crosslinking reveals the relative orientation of the cytoplasmic and membrane domains of Band
376 3, a model for Band 3 tetramerization, a more extensive Band 3-ankyrin interface, and cross-
377 linking sites to Glycophorin A, protein 4.1, and protein 4.2.
- 378 34. Shnitsar V, Li J, Li X, Calmettes C, Basu A, Casey JR, Moraes TF, Reithmeier RAF: **A substrate**
379 **access tunnel in the cytosolic domain is not an essential feature of the solute carrier 4**
380 **(SLC4) family of bicarbonate transporters.** *J. Biol. Chem.* 2013, **288:33848–33860.**
- 381 35. Puchulu-Campanella E, Turrini FM, Li Y-H, Low PS: **Global transformation of erythrocyte**
382 **properties via engagement of an SH2-like sequence in band 3.** *Proc Natl Acad Sci USA* 2016,
383 **113:13732–13737.**
- 384 ** Identification of a SH2-like sequence in short helical segment of Band 3 linking the gate and core
385 domains that regulates anion transport via a phosphorylation-dependent mechanism. Further,
386 engagement of this SH2-like sequence by the cytosolic domain displaces ankyrin, thereby
387 rupturing the Band 3-spectrin linkage and resulting in decreased membrane strength.
- 388 36. Pantaleo A, Kesely KR, Pau MC, Tsamesidis I, Schwarzer E, Skorokhod OA, Chien HD, Ponzi
389 M, Bertuccini L, Low PS, et al.: **Syk inhibitors interfere with erythrocyte membrane**
390 **modification during P falciparum growth and suppress parasite egress.** *Blood* 2017,
391 **130:1031–1040.**
- 392 37. Gupta K, Donlan JAC, Hopper JTS, Uzdavinys P, Landreh M, Struwe WB, Drew D, Baldwin AJ,
393 Stansfeld PJ, Robinson CV: **The role of interfacial lipids in stabilizing membrane protein**

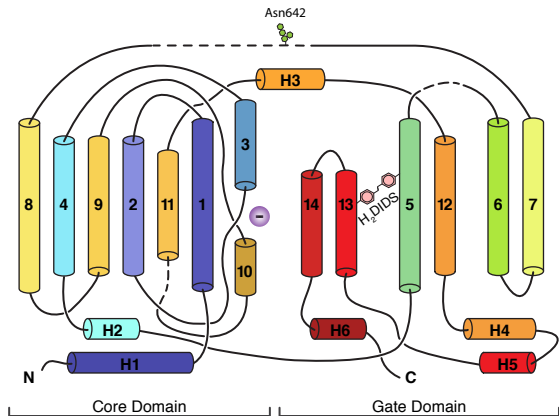
- 394 **oligomers.** *Nature* 2017, **541**:421–424.
- 395 * Highlights key role of lipids at the interface between membrane proteins subunits.
- 396 38. Macara IG, Cantley LC: **Interactions between Transport Inhibitors at the Anion Binding**
397 **Sites of the Band 3 Dimer.** *Biochemistry* 1981, **20**:5095–5105.
- 398 39. Groves JD, Tanner MJ: **Co-expressed complementary fragments of the human red cell anion**
399 **exchanger (band 3, AE1) generate stilbene disulfonate-sensitive anion transport.** *Journal of*
400 *Biological Chemistry* 1995, **270**:9097–9105.
- 401 40. Groves JD, Wang L, Tanner MJ: **Functional reassembly of the anion transport domain of**
402 **human red cell band 3 (AE1) from multiple and non-complementary fragments.** *FEBS Lett*
403 1998, **433**:223–227.
- 404 41. Thevenin BJ, Low PS: **Kinetics and regulation of the ankyrin-band 3 interaction of the**
405 **human red blood cell membrane.** *Journal of Biological Chemistry* 1990, **265**:16166–16172.
- 406 42. Bruce LJ, Ring SM, Anstee DJ, Reid ME, Wilkinson S, Tanner MJ: **Changes in the blood group**
407 **Wright antigens are associated with a mutation at amino acid 658 in human erythrocyte**
408 **band 3: a site of interaction between band 3 and glycophorin A under certain conditions.**
409 *Blood* 1995, **85**:541–547.
- 410 43. Toye AM, Ghosh S, Young MT, Jones GK, Sessions RB, Ramaugé M, Leclerc P, Basu J,
411 Delaunay J, Tanner MJA: **Protein-4.2 association with band 3 (AE1, SLCA4) in Xenopus**
412 **oocytes: effects of three natural protein-4.2 mutations associated with hemolytic anemia.**
413 *Blood* 2005, **105**:4088–4095.
- 414 44. Bruce LJ, Beckmann R, Ribeiro ML, Peters LL, Chasis JA, Delaunay J, Mohandas N, Anstee DJ,
415 Tanner MJA: **A band 3–based macrocomplex of integral and peripheral proteins in the RBC**
416 **membrane.** *Blood* 2003, **101**:4180–4188.
- 417 45. Satchwell TJ, Bell AJ, Hawley BR, Pellegrin S, Mordue KE, van Deursen CTBM, Braak NH-T,
418 Huls G, Leers MPG, Overwater E, et al.: **Severe Ankyrin-R deficiency results in impaired**
419 **surface retention and lysosomal degradation of RhAG in human erythroblasts.**
420 *Haematologica* 2016, **101**:1018–1027.
- 421 46. Genetet S, Desrames A, Chouali Y, Ripoche P, Lopez C, Mouro-Chanteloup I: **Stomatin**
422 **modulates the activity of the Anion Exchanger 1 (AE1, SLC4A1).** *Sci. Rep.* 2017, **7**:46170.
- 423 47. Malik S, Sami M, Watts A: **A Role for Band 4.2 in Human Erythrocyte Band 3 Mediated**
424 **Anion Transport.** *Biochemistry* 1993, **32**:10078–10084.
- 425 48. Hsu K, Lee T-Y, Periasamy A, Kao F-J, Li L-T, Lin C-Y, Lin H-J, Lin M: **Adaptable**
426 **interaction between aquaporin-1 and band 3 reveals a potential role of water channel in**
427 **blood CO2 transport.** *FASEB J* 2017, doi:10.1096/fj.201601282R.
- 428 49. Zhao J, Benlekbir S, Rubinstein JL: **Electron cryomicroscopy observation of rotational states**

- 429 **in a eukaryotic V-ATPase.** *Nature* 2015, **521**:241–245.
- 430 50. Mazhab-Jafari MT, Rohou A, Schmidt C, Bueler SA, Benlekbir S, Robinson CV, Rubinstein JL:
431 **Atomic model for the membrane-embedded VO motor of a eukaryotic V-ATPase.** *Nature*
432 2016, **539**:118–122.
- 433 51. Fowler PW, Sansom MSP, Reithmeier RAF: **Effect of the Southeast Asian Ovalocytosis**
434 **Deletion on the Conformational Dynamics of Signal-Anchored Transmembrane Segment 1 of**
435 **Red Cell Anion Exchanger 1 (AE1, Band 3, or SLC4A1).** *Biochemistry* 2016, **56**:712–722.
- 436 52. Badior KE, Alka K, Casey JR: **SLC4A11 Three-Dimensional Homology Model Rationalizes**
437 **Corneal Dystrophy-Causing Mutations.** *Hum. Mutat.* 2017, **38**:279–288.
- 438 * A 3-D model of SLC4A11 based on the structure of Band 3 allowed localization of disease-
439 causing mutations within critical regions of the protein and provided the structural context for
440 studies of the effects of the mutations on functional expression of the transporter.
- 441
- 442 53. Rapp C, Bai X, Reithmeier RAF: **Molecular analysis of human solute carrier SLC26 anion**
443 **transporter disease-causing mutations using 3-dimensional homology modeling.** *Biochimica*
444 *et Biophysica Acta (BBA) - Biomembranes* 2017, **1859**:2420–2434.
- 445 54. Bassot C, Minervini G, Leonardi E, Tosatto SCE: **Mapping pathogenic mutations suggests an**
446 **innovative structural model for the pendrin (SLC26A4) transmembrane domain.** *Biochimie*
447 2017, **132**:109–120.
- 448

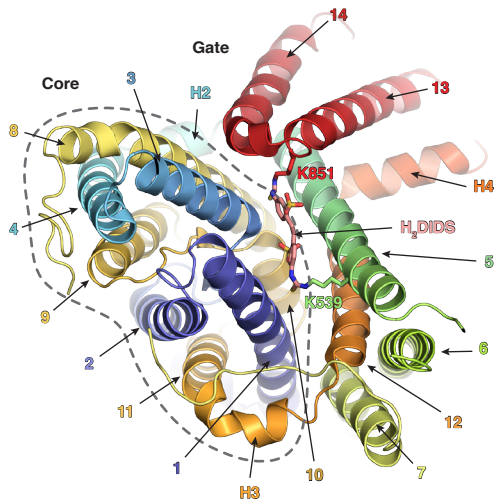
(a) Figure 2



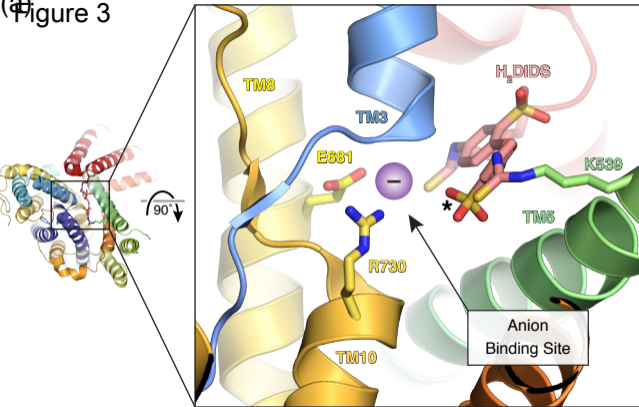
(b)



(c)



(a) Figure 3



(b)

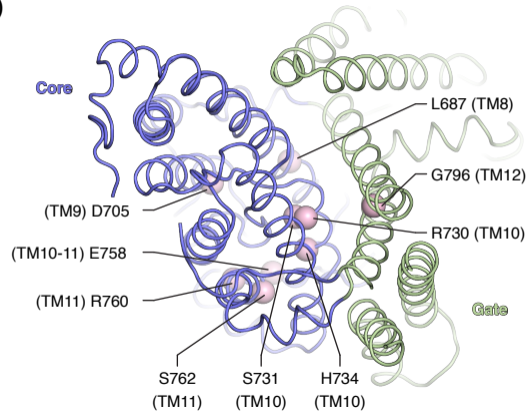
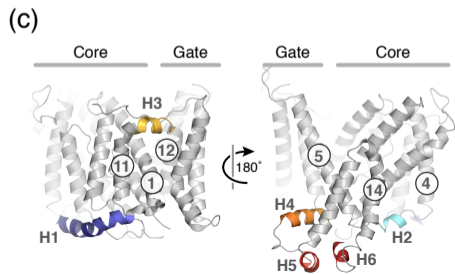
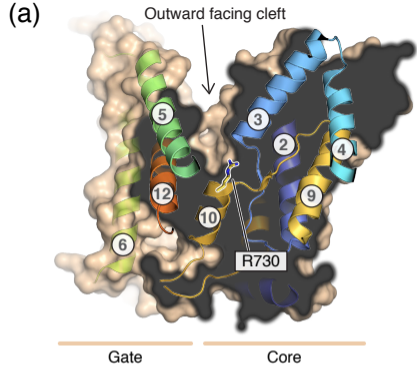
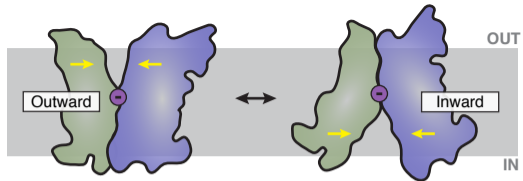


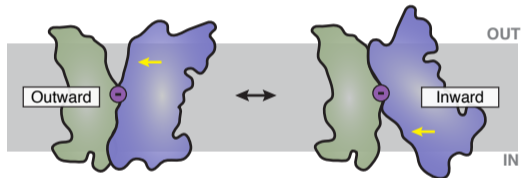
Figure 4



(b) Rocking Switch - Both domains rock



Rocking Bundle - One domain rocks against a rigid scaffold



Elevator - One domain rocks while translocating substrate

